IEEE Photonics Journal
An IEEE Photonics Society Publication

Demonstration of OCDM Coder and Variable Bandwidth Filter Using Parallel Topology of Quadruple Series Coupled Microring Resonators

Volume 3, Number 1, February 2011

Kengo Tanaka
Yasuo Kokubun, Fellow, IEEE

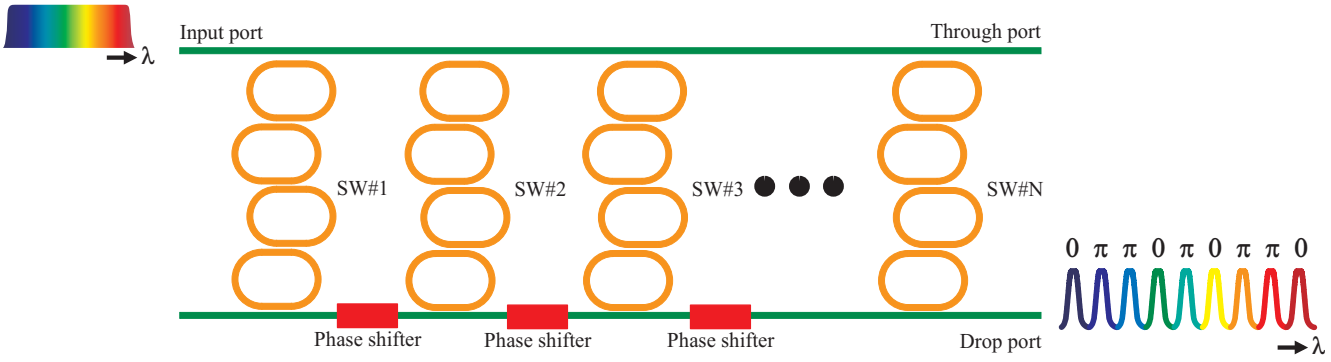

DOI: 10.1109/JPHOT.2010.2096804
1943-0655/$26.00 ©2010 IEEE

Demonstration of OCDM Coder and Variable Bandwidth Filter Using Parallel Topology of Quadruple Series Coupled Microring Resonators

Kengo Tanaka and Yasuo Kokubun, *Fellow, IEEE*

Department of Electrical and Computer Engineering, Graduate School of Engineering, Yokohama National University, Yokohama 240-8501, Japan

DOI: 10.1109/JPHOT.2010.2096804
1943-0655/$26.00 ©2010 IEEE

Manuscript received October 29, 2010; revised November 25, 2010; accepted November 27, 2010. Date of publication December 2, 2010; date of current version January 24, 2011. Corresponding author: Y. Kokubun (e-mail: ykokubun@ynu.ac.jp).

Abstract: The quadruple series coupled microring resonator (MRR) can realize a boxlike spectral response and lower adjacent channel crosstalk. Utilizing these features, we demonstrated the element of Optical Code Division Multiplexing (OCDM) coding circuit using two wavelength selective switches (WSSs) consisting of quadruple series coupled MRRs laid out in parallel topology and a phase shifter incorporated in the one arm between them. In addition, a digitally variable bandwidth filter was successfully demonstrated using the same circuit as the OCDM coder.

Index Terms: Microring resonator, series coupling, wavelength selective switch, optical code division multiplexing, variable bandwidth filter.

1. Introduction

The optical Code Division Multiplexing (OCDM) system is a promising technology to expand the transmission capacity and flexibility of optical fiber network in the future [1]. In the OCDM system, each channel is assigned a different optical code. In the receiver, the channel is decoded as the correlated signal by pattern matching.

Previously, we demonstrated a hitless wavelength selective switch (WSS) using individual Thermo-Optic tuning of series coupled microring resonators (MRRs) [2], [3]. In addition, we demonstrated an OCDM coder using double series coupled MRRs [4]. However, the roll-off of the spectral response was not steep enough to our satisfaction. In this study, we aimed at demonstrating the element of the OCDM coder using the quadruple series coupled MRR enabling a boxlike spectral response.

As we introduce the element of OCDM coder using the parallel topology of quadruple series coupled MRR, the spectral response is made boxlike without additional loss, and the pass bands are arranged with arbitrary close spacing, in contrast with the OCDM coder using arrayed waveguide gratings (AWGs) [5], [6]. Even in [1], which used the parallel layout of fourth-order series coupled microrings, the 3-dB bandwidths of 8 GHz were arranged with the spacing of 10 GHz, and therefore, the window of 2 GHz remained unused. On the other hand, we found that when the 3-dB bandwidths of the parallel layout of the series coupled microrings are continuously laid out, the overall bandwidth is flattened, and the efficiency of spectrum usage can be improved. Thus, we have improved the

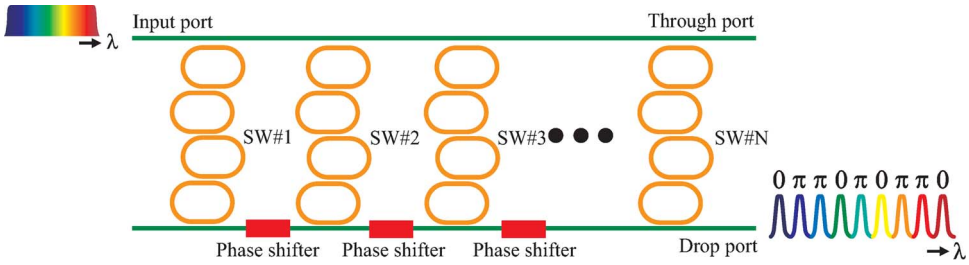

Fig. 1. Conceptual schematic of OCDM coding.

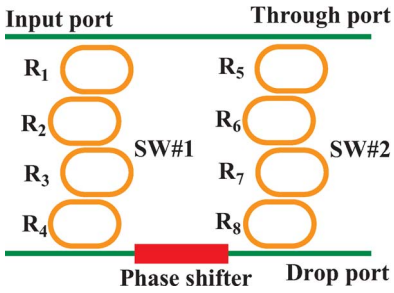

Fig. 2. Schematic of OCDM coding circuit using tunable quadruple series coupled MRRs.

Fig. 3. Schematic of equivalent MZI.

efficiency of spectrum usage by arranging the wavelength channels of the OCDM coder so that the 3-dB bandwidths are continuously laid out and realized bandwidth variable filter through switching individual elements.

2. Principle

As shown in Fig. 1, an OCDM coding circuit was constructed by the parallel layout of multiple quadruple series coupled MRRs and the phase shifters utilizing the Thermo-Optic effect incorporated into the one arm located between the switch elements. Coding can be realized by controlling the phase difference ($\Delta\phi = 0$ or π rad) at the state in which resonant wavelengths of switches are arranged so that their 3-dB bandwidths are continuously laid out when the incident light on the input port is transmitted to the drop port.

We can explain the principle of coding using an elemental circuit that consists of two switch elements, as shown in Fig. 2. Now, let us suppose the wavelength at which two spectral responses cross over when resonant wavelengths of SW#1 and SW#2 are arranged so that their 3-dB bandwidths are continuously laid out. Then, this circuit is equivalent to a Mach–Zehnder Interferometer (MZI) at this wavelength, as shown in Fig. 3. In the equivalent MZI, first, the incident light on the input port is divided into two arms. Next, if the phase difference between them is in phase, they are combined and transmitted to the lower port (drop port). Consequently, as shown in Fig. 4, the drop port response becomes flat and has double bandwidth. On the other hand, if out of phase, they are transmitted to the upper port (through port), and a dip appears at the center of spectrum. Accordingly, this device can serve as the coding circuit since two states can be differentiated by observing the existence of the dip.

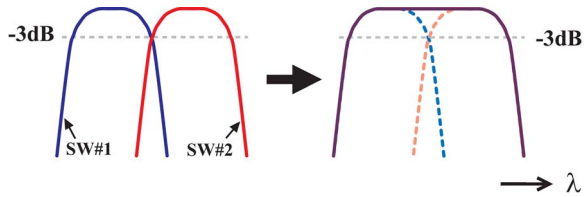

Fig. 4. Change of spectral shape at the cross over wavelength.

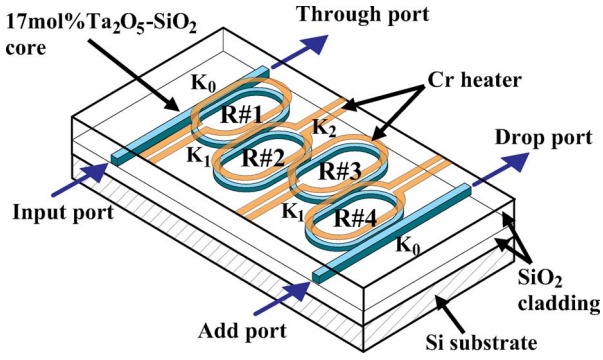

Fig. 5. Perspective view of WSS using quadruple series coupled MRRs.

When the phase difference $\Delta\phi = 0$ rad, by arranging the pass bands of SW#1 and SW#2 so that their 3-dB bandwidths are continuously laid out, the bandwidth can be doubled, as shown in Fig. 4. The ON/OFF switching of switch elements enables the bandwidth to be varied digitally by an integer multiple of spectral response of each switch element. By this means, this device can serve as the digitally variable bandwidth filter by the ON/OFF switching of switch elements. If the 3-dB bandwidths are arranged to be overlapped with each other, the overlapped band appears as the stop band in the drop port response. This is because the wavelength in the overlapped band is transmitted to the drop port of the first switch and returns again to the through port of the second switch. Therefore, the overall bandwidth cannot be varied continuously but can be varied digitally by an integer multiple of the 3-dB bandwidth of each switch element.

3. Device Fabrication

The structure of the hitless WSS is shown in Fig. 5. The core and the upper cladding materials were sputter deposited 17 mol%Ta_2O_5-SiO_2 (n = 1.660 @λ = 1550 nm) and SiO_2 (n = 1.445 @ λ = 1550 nm), respectively. The busline waveguide and MRR were laterally coupled (single-layer structures). The ring resonators were racetrack shaped, and the coupling efficiency was controlled by the overlap length of the straight portion of the racetrack resonators. The so-called clothoid curve was introduced to the curved sections of the microrings. The core height and width were 1.3 μm and 1.3 μm, respectively, which satisfies the single-mode propagation condition. The round-trip length of the racetrack resonator was 611 μm, which corresponds to the free spectrum range (FSR) of 2.22 nm. Fig. 6 shows the microscopic photo of the fabricated device after heater formation.

By applying current to the microheaters formed on the MRRs, the resonant wavelengths of the series-coupled MRRs can be individually controlled, and this device can operate as a hitless WSS. When all resonant wavelengths are matched, the wavelength channel is transmitted to the drop port (ON-state). Otherwise, no resonant peak appears at the drop port (OFF-state). In addition to the hitless WSS, we formed a microheater on one arm of the busline waveguide between switch elements to serve as a phase shifter.

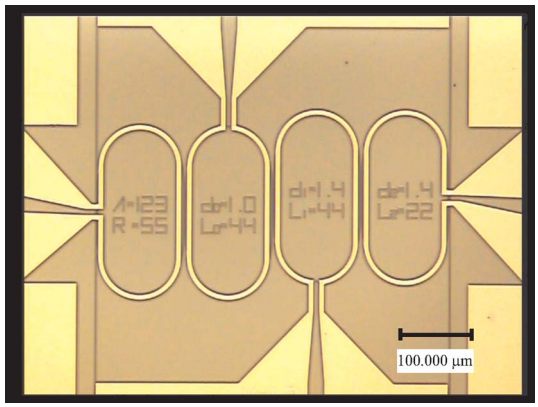

Fig. 6. Fabricated device after heater formation by laser microscope.

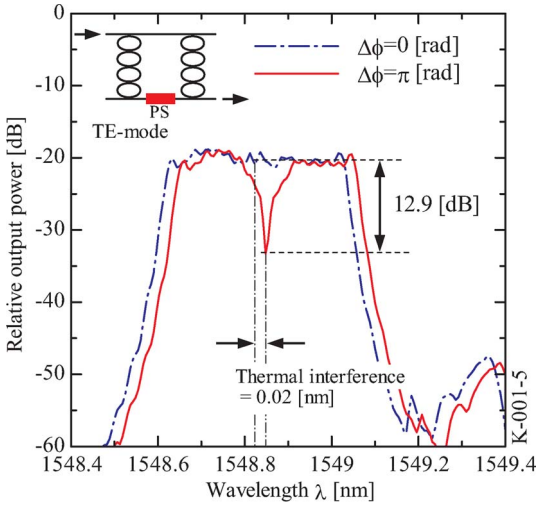

Fig. 7. Change of drop port response by phase shift.

4. Experiment

4.1. OCDM Coding Characteristics

In the initial state, when no electric current was applied, the resonant wavelengths of the individual microrings were slightly different due to the fabrication error. First, we put both switches in the ON-state by applying current. Then, the resonant wavelength of SW#2 was shifted to a longer wavelength so that the 3-dB bandwidths of SW#1 and SW#2 were arranged continuously. The phase between two arms was controlled ($\Delta\phi = 0$ or π rad). The result is shown in Fig. 7.

By applying electric current to the phase shifter, a dip appeared at the center of the drop port response. The dip reached a maximum depth of -12.9 dB when the supplied current was 16 mA (525 mW) for transverse electric (TE) polarization, which corresponds to the phase difference of π rad. Similar results were also observed for transverse magnetic (TM) polarization. For TM polarization, the dip reached a maximum depth of -18.7 dB when the supplied current was 16 mA (525 mW). Then, increasing the current further, the dip depth gradually decreased. This means that the phase difference changed from π rad to 2π rad, as shown in Fig. 8. It is seen from Fig. 8 that the electric power required to achieve the phase shift of π was the same for TE and TM polarizations.

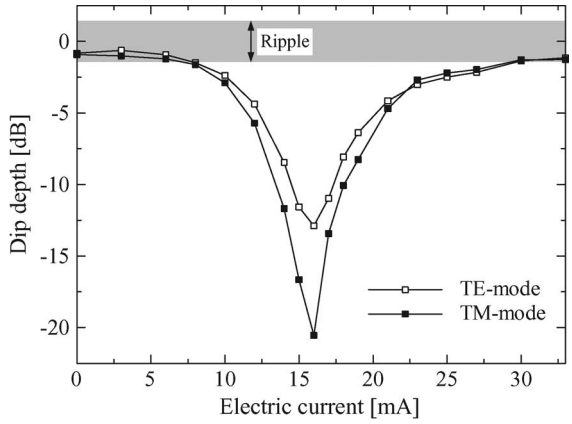

Fig. 8. Variation of dip depth of drop port response versus electric current.

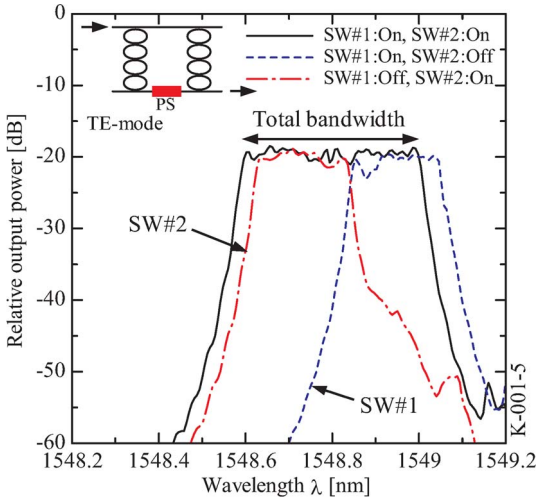

Fig. 9. Bandwidth variable characteristics of drop port response.

The reason why the dip depth did not reach the minus infinity is attributed to the limit of resolution of the spectrum analyzer (6 pm).

These results demonstrate the element of an OCDM coder corresponding to one bit.

4.2. Bandwidth Variable Characteristics

On the other hand, the bandwidth of overall spectral response was doubled (0.42 nm) by shifting the resonant wavelength of SW#2 to continuously line up the 3-dB bandwidths of SW#1 (0.21 nm) and SW#2 (0.21 nm). By the ON/OFF switching of SW#1 and SW#2, the overall bandwidth was digitally controlled, as shown in Fig. 9. As a result, the shape factor was increased from 0.83 to 0.91. This result demonstrates a variable bandwidth filter. Similar results were also observed for TM polarization.

5. Conclusion

An OCDM coding circuit in the spectral region was realized by a parallel layout of quadruple series-coupled MRRs and the phase difference control between switch elements. A digitally variable bandwidth filter with a bandwidth, that is, a multiple of that of the single switch element, was also successfully demonstrated.

Acknowledgment

This work was supported in part by the Strategic Information and Communication R&D Promotion Programme (SCOPE) from the Ministry of Internal Affairs and Communications.

References

[1] A. Agarwal, P. Toliver, R. Menendez, S. Etemad, J. Jackel, J. Young, T. Banwell, B. E. Little, S. T. Chu, W. Chen, W. Chen, J. Hryniewicz, F. Johnson, D. Gill, O. King, R. Davidson, K. Donovan, and P. J. Delfyett, "Fully programmable ring-resonator-based integrated photonic circuit for phase coherent applications," *J. Lightw. Technol.*, vol. 24, no. 1, pp. 77–87, Jan. 2006.

[2] Y. Goebuchi, T. Kato, and Y. Kokubun, "Fast and stable wavelength selective switch using double-series coupled dielectric microring resonator," *IEEE Photon. Technol. Lett.*, vol. 18, no. 3, pp. 538–540, Feb. 2006.

[3] Y. Goebuchi, T. Kato, and Y. Kokubun, "Multiwavelength and multiport hitless wavelength-selective switch using series-coupled microring resonators," *IEEE Photon. Technol. Lett.*, vol. 19, no. 9, pp. 671–673, May 2007.

[4] Y. Goebuchi, M. Hisada, T. Kato, and Y. Kokubun, "Optical cross-connect circuit using hitless wavelength selective switch," *Opt. Express*, vol. 16, no. 2, pp. 535–548, Jan. 2008.

[5] J. Cao, R. G. Broeke, C. Ji, Y. Du, N. Chubun, P. Bjeletich, S. J. B. Yoo, F. Olsson, S. Lourdudoss, and P. L. Stephan, "A monolithic ultra-compact InP O-CDMA encoder with planarization by HVPE regrowth," presented at the Optical Fiber Commun. Conf./National Fiber Optic Engineers Conf., Anaheim, CA, 2005, Paper OFL6.

[6] F. Moritsuka, N. Wada, T. Sakamoto, T. Kawanishi, Y. Komai, S. Anzai, M. Izutsu, and K. Kodate, "Multiple optical code-label processing using multi-wavelength frequency comb generator and multi-port optical spectrum synthesizer," *Opt. Express*, vol. 15, no. 12, pp. 7515–7521, Jun. 2007.